Journal of Alloys and Compounds 509 (2011) 2503–2509

Contents lists available at ScienceDirect

Journal of Alloys and Compounds

journal homepage: www.elsevier.com/locate/jallcom

Synthesis and characterization of in situ Al–AlN composite by nitrogen gas bubbling method

S.S. Sreeja Kumari, U.T.S. Pillai*, B.C. Pai

Materials and Minerals Division, National Institute for Interdisciplinary Science and Technology (CSIR), Thiruvananthapuram, Industrial Estate PO, Pappanamcode, Trivandrum 695 019, Kerala, India

ARTICLE INFO

Article history:
Received 28 September 2010
Received in revised form 4 November 2010
Accepted 10 November 2010
Available online 26 November 2010

Keywords:
Al–AlN composites
In situ method
Microstructure
Scanning electron microscopy
X-ray diffraction

ABSTRACT

In situ Al–AlN composite with and without Mg addition was synthesized by nitrogen gas bubbling method. The morphology of the particles was found to be hexagonal by SEM and TEM. The size of the AlN particles was found to be in the range from nano, submicron to a few microns. XRD analysis of the extracted particles confirmed the formation of AlN in the melt. Mg addition enhanced the nitridation rate and formed network of interconnected AlN particles. Hardness of the composite is significantly increased by the hard AlN particles. Further, the mechanism of formation of AlN particles inside the molten aluminium by gas bubbling is discussed.

1. Introduction

In situ metal matrix composites (MMCs) are a kind of novel composites, in which the reinforcements are formed within the parent phase by controlling melt growth, chemical reactions between elements or between element and compound, transformation and deformation during the composite fabrication [1]. Among the various in situ routes, the gas bubbling method, in which the reinforcing particles are formed from the reaction between molten metal and bubbling gas, has great advantages. Gas injection processing was first developed by Koczak and Kumar [2], in which reactive gases are introduced into the melt and the reinforcement is formed through the reaction between the gas or its decomposition product and the melt or its alloying elements. The in situ reaction could form uniformly distributed fine reinforcing particles, and very clear interfaces between particles and matrix. So it is a very attractive processing for the production of in situ composites.

Various composites of Al/TiC, Al/TaC, Al/TiN, Al/Al_3Ti–AlN, Al/TiC–AlN, Al/Al_2O_3 and Al/Al_2O_3–TiC have been fabricated by this process [2–9]. In recent years, however, Al–AlN composite has received considerable attention [6,10]. Aluminium nitride is a novel ceramic material. It crystallizes in the hexagonal wurtzite structure. It has a large band gap of 6.3 eV that makes it a good insulating material. It has a low density ($3.026\,g/cm^3$), a low coefficient of thermal expansion ($4.5 \times 10^{-6}\,K^{-1}$, in the temperature range 293–673 K) and a very good thermal conductivity ($110–170\,W\,m^{-1}\,K^{-1}$) [11]. It is resistant to thermal shock and can absorb a high level of energy when exposed to high pressure and strain rates [12]. Thus, it has attractive properties for widespread applications such as electronic substrates, protective coating, optoelectronic parts, heat sinks, cutting tools, high-power chips and fillers for polymer and glass materials. Not only can AlN enhance the modulus, strength, hardness, wear resistance and refractory nature of aluminium alloy matrix, as SiC or Al_2O_3 does, but it has also other advantages. AlN is much more wettable to aluminium compared to Al_2O_3. From stability viewpoint, AlN reinforcement does not react or decompose in molten aluminium, as SiC does. Therefore, the interfacial reactions and problems associated with poor interface, which have proven to be a significant drawback of Al/SiC or Al/Al_2O_3 composites, do not exist in Al/AlN alloy composites [6]. However, Al/AlN composite has not yet been widely commercialized because of the high cost of fine AlN powders.

In recent years, there have been attempts to produce aluminium nitride (AlN) or AlN composites utilizing the reaction between the molten Al and the reaction gas [13]. The formation of Al–AlN composites has not been successful by means of this method for a long time. It was thought that formation of AlN by bubbling nitrogen gas was not feasible due to the limitation of intrinsic kinetics such as passivation at the interface [6]. However, works by Zheng and Reddy [14–18] and Seon Shin et al. [10] have shown that by process optimization Al–AlN composites could be obtained using this technique. Further, the mechanism of AlN formation in the pro-

---

* Corresponding author. Tel.: +91 471 2515236; fax: +91 471 2491712.
E-mail address: utspillai@rediffmail.com (U.T.S. Pillai).

0925-8388/$ – see front matter © 2010 Elsevier B.V. All rights reserved.
doi:10.1016/j.jallcom.2010.11.065

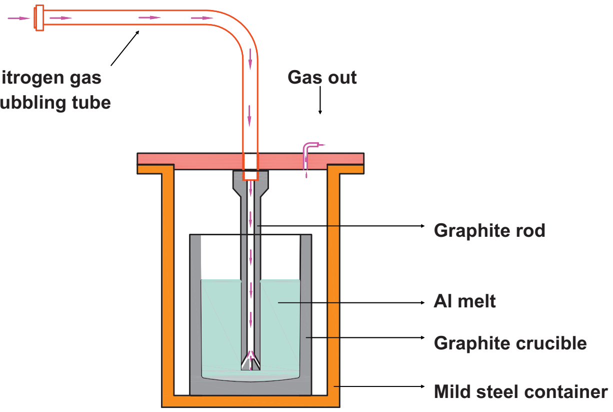

Fig. 1. Experimental set-up for the synthesis of in situ Al–AlN composite.

cess of gas/melt reaction has not been well explained. This paper presents the synthesis of in situ Al/AlN composite by passing high purity nitrogen gas through pure Al and Al–Mg melt at different gas flow rates. The possible reaction mechanisms were also discussed. The composites fabricated have been characterized for their microstructure and microhardness.

2. Materials and methods

The schematic diagram of the experimental set-up is shown in Fig. 1. Experiments were carried out in a resistance furnace. Graphite crucible was used for melting aluminium. This was kept inside a mild steel container which was closed at the bottom end and sealable at the top end. The gas bubbling tube made out of graphite with holes around it with nozzle diameter of 3 mm was submerged into the melt up to the bottom of the crucible during the bubbling. Pure Al (EC Grade with purity 99.75% Al) was used as the starting material. Experiments were also carried out with 4 wt% Mg (elemental form) addition. Nitrogen gas of high purity (99.997% with <6 ppm O_2) was used. The total weight of Al is about 250 g. The nitrogen gas was bubbled at 1173 K, into the melt through the lance. The reaction temperature was controlled at 1173 ± 5 K and the bubbling time was varied from 2 to 4 h. The gas flow rate [0.4 and 0.6 liter per min (lpm)] was maintained by a flow meter. After the desired reaction time, the melt was cooled to 1013 K and manually stirred, skimmed and then poured into a preheated (473 K) permanent mould.

The specimens for micro-structural observation were cut from the castings (20 mm diameter × 120 mm length). The microstructures of the samples were studied in an optical microscope (Leitz Metalloplan), and a scanning electron microscope (SEM) coupled with an energy dispersive X-ray spectrometer. A Leico 2001 image analyzer was used in conjunction with the optical microscope for finding the volume fraction of the AlN particles. In order to examine the size and morphology of the reaction products in a detailed manner, the reaction products were extracted from the permanent mould casting by leaching out the Al matrix using NaOH (10%). Then the settled particles were dried and examined by X-ray diffraction analyses, SEM/EDS and Transmission Electron Microscope (TEM). The CLEMEX Micro Hardness Tester was used to determine the microhardness (Vickers Hardness Number, VHN) at test load of 25 g and dwell time of 13 s. An average of 10–15 readings was taken as a measure of the representative hardness of the matrix.

3. Results

3.1. Microstructure

Fig. 2 shows the optical micrograph of Al–AlN composite formed from pure Al at temperature 1173 K by passing high purity N_2 gas (gas flow rate 0.4 lpm) for 2 h. It is seen that the AlN formed is uniformly distributed in the matrix. The volume fraction of the AlN formed was found to be 2% and the average size of the particles is ~4 μm by image analysis (average of particles in eight fields in the microstructure).

Figs. 3 and 4 show the optical and SEM micrograph of the permanent mould cast Al–4Mg alloy sample (gas flow rate 0.4 lpm) respectively. It is seen that AlN particles are in larger amounts and the size of the particles range from micron, submicron and to nanolevels. In this case, the particles are interconnected and seen as network of particles in the grain boundaries. The volume fraction of the AlN particles by image analysis could not be done in these samples because the particles are very small and are seen in network form. However, these individual particles are seen at higher magnification by SEM (Fig. 4). The extracted particles from this sys-

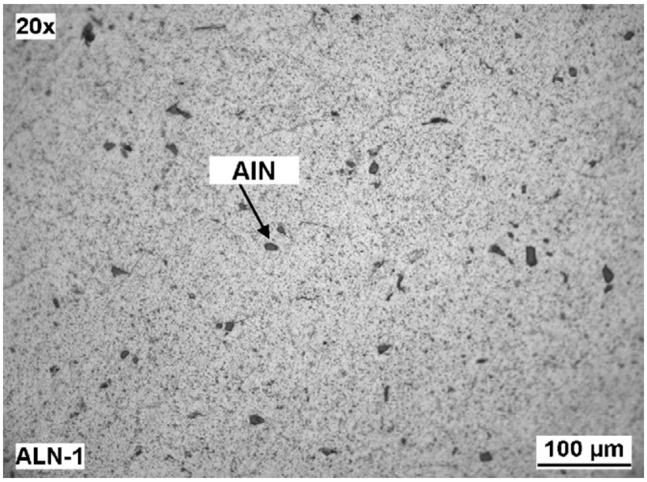

Fig. 2. Optical micrographs of the in situ Al–AlN composite formed from pure Al after 2 h reaction (gas flow rate: 0.4 lpm).

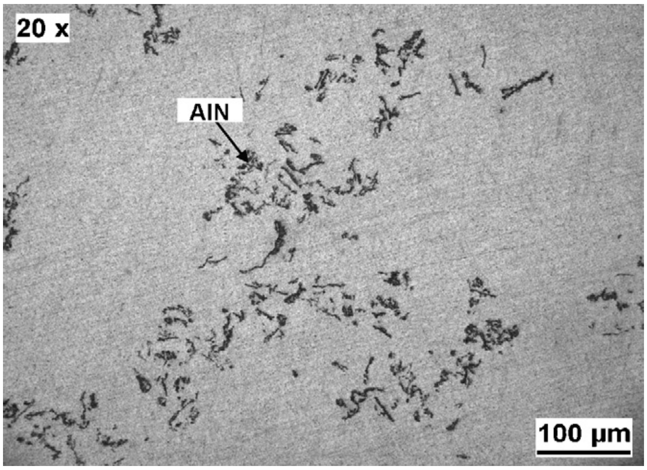

Fig. 3. Optical micrographs of the in situ Al–4Mg–AlN composite after 4 h reaction (gas flow rate: 0.4 lpm).

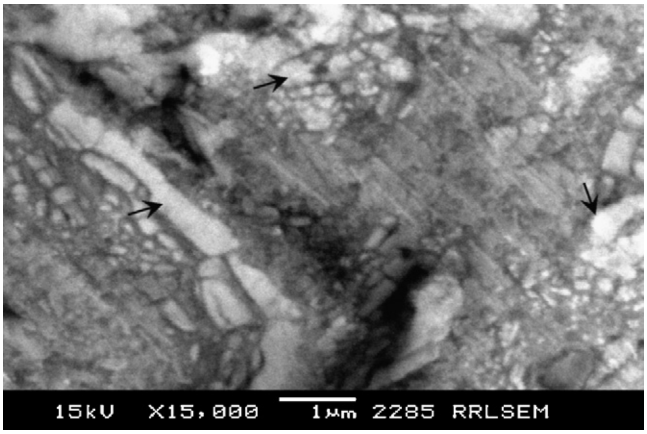

Fig. 4. SEM micrographs of the in situ Al–4Mg–AlN composite after 4 h reaction (gas flow rate: 0.4 lpm).

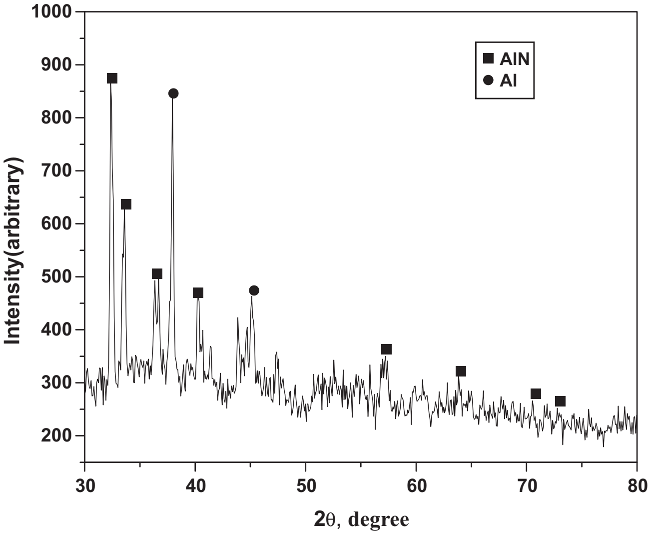

Fig. 5. XRD pattern of the extracted particles from the Al–AlN sample after 4 h reaction (close to JCPDS No.: 25-1133).

tem have been analyzed by XRD which shows that these particles are AlN (Fig. 5). Fig. 6 shows the SEM photograph and EDS analysis of the extracted particles from Al–4Mg alloy system. The morphology of the particles was found to be hexagonal. It should be noted that the deviation of the atomic ratio of Al/N from stoichiometry could be due to the factors, such as the analysis error of EDS for light elements, in-completion of the nitridation, etc. Further, the small amount of magnesium and carbon detected in the extracted particles is believed to be the impurities come from crucible and lance. The nano-size and hexagonal morphology of the AlN particles have been further confirmed by TEM (Fig. 7).

Figs. 8 and 9 show the optical and SEM micrographs of in situ Al–4Mg–AlN composite after 4 h reaction (gas flow rate: 0.6 lpm). It is seen that with the increase in the gas flow rate from 0.4 to 0.6 lpm more number of fine particles (mostly nano) were obtained. However, in addition to this some other phases have been seen (shown by arrows in Fig. 8(b–d). This may be $MgAl_2O_4$ spinel layer formed due to the reaction of MgO with Al as reported earlier which needs detailed investigation further.

3.2. Microhardness

Fig. 10 shows the Vickers' micro-hardness values recorded from different locations in the microstructure of the composite samples. Compared to the hardness [20] of pure Al, the hardness values of the in situ composites have been significantly increased. It is seen that Mg added samples with longer reaction time show significantly higher hardness compared to that without Mg and less reaction time. Similarly, with same Mg content and reaction time but at higher gas flow rate, the hardness is significantly increased. As seen in the microstructure, this is due to larger amounts of AlN formed in the two cases.

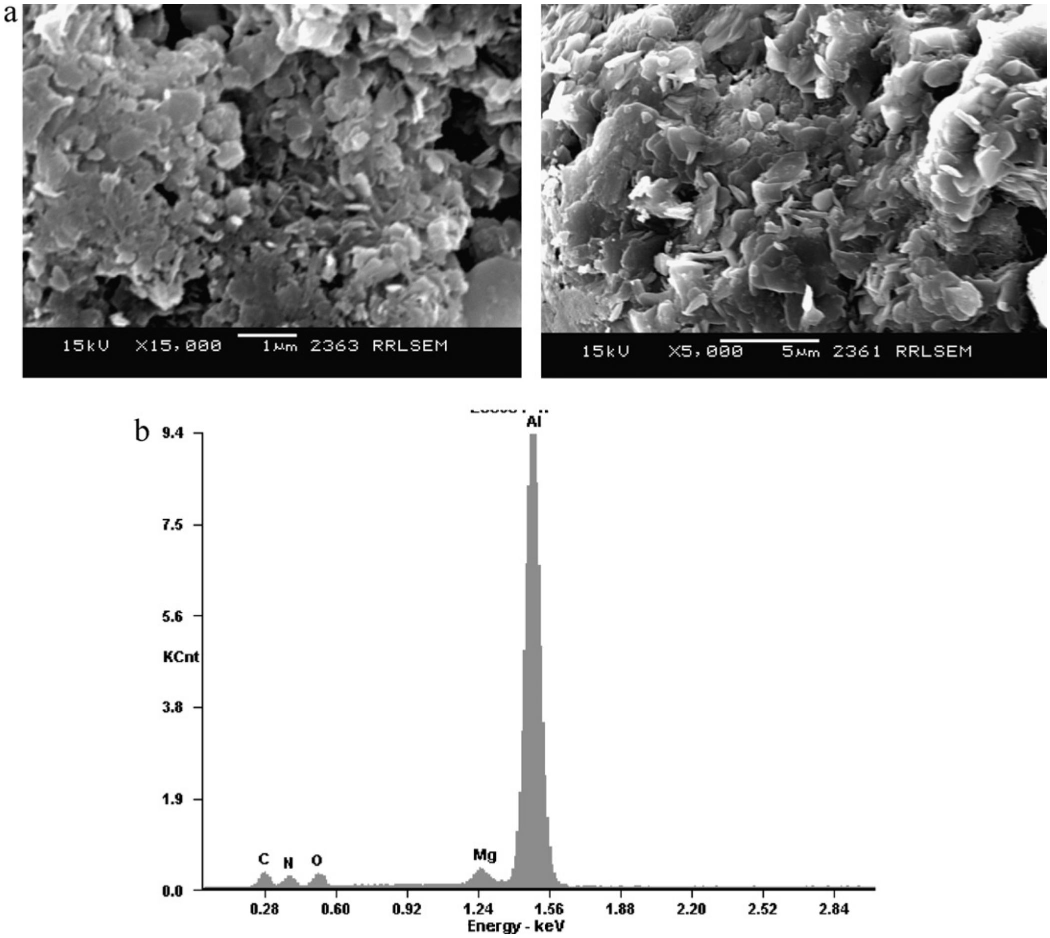

Fig. 6. (a) SEM photograph showing morphology of the extracted AlN particles from Al–AlN in situ composite and (b) EDS showing distributions of Al, N, Mg, C and O in the phase.

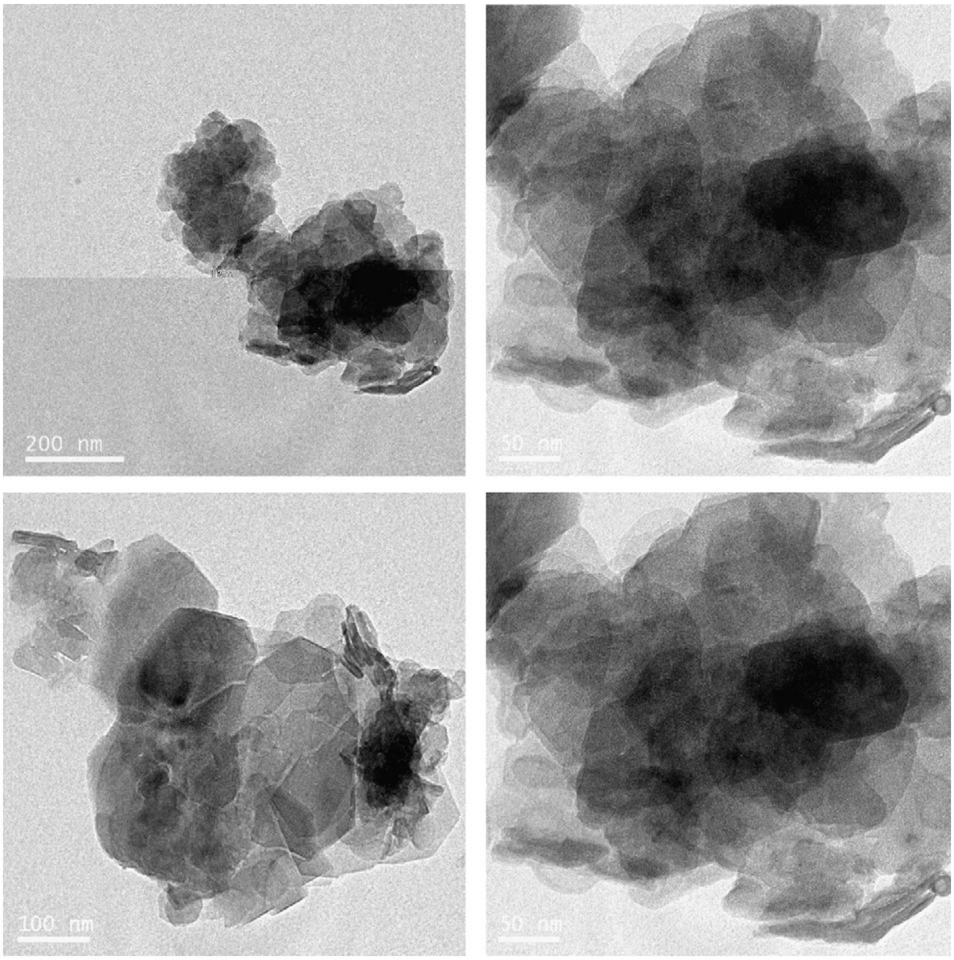

Fig. 7. TEM photographs showing hexagonal morphology of the extracted AlN particles from Al–AlN in situ composite.

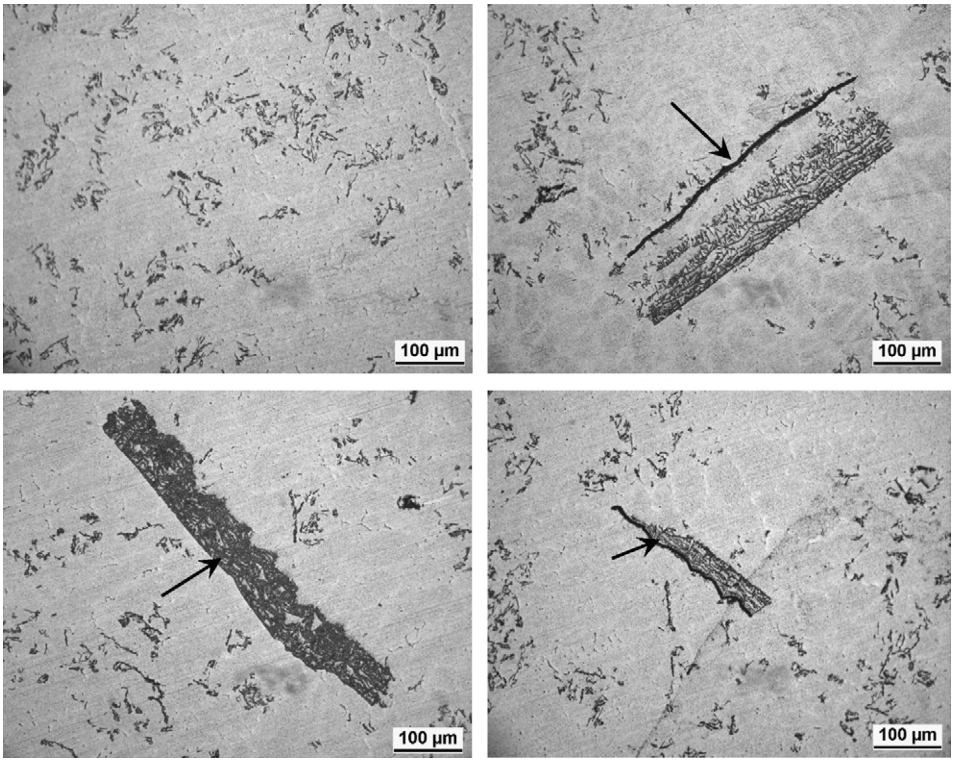

Fig. 8. Optical micrographs of the in situ Al–4Mg–AlN composite after 4 h reaction (gas flow rate: 0.6 lpm).

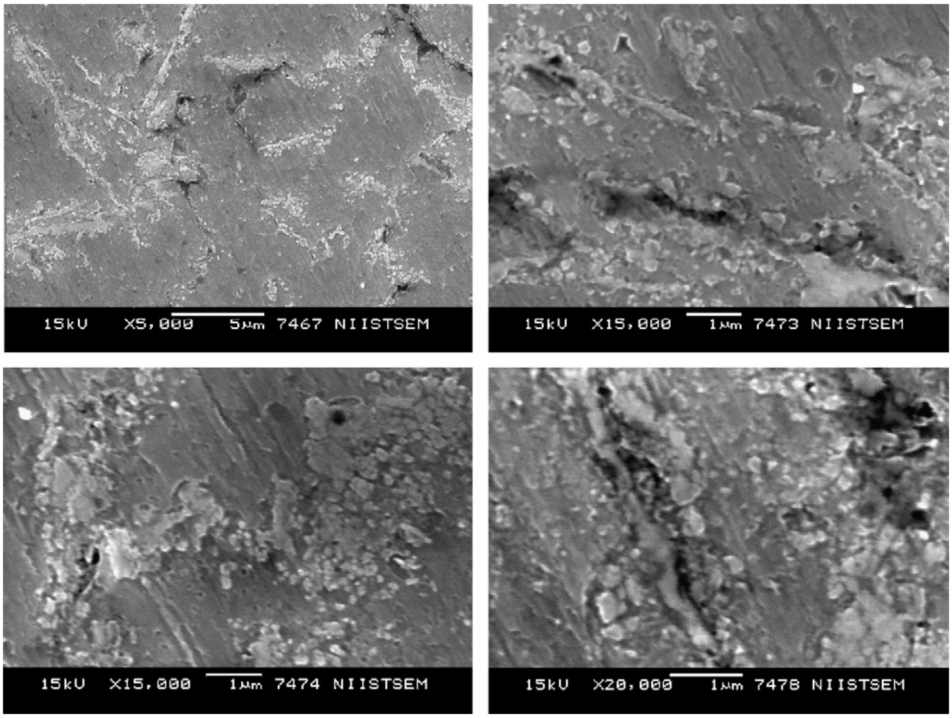

Fig. 9. SEM micrographs of the in situ Al–4Mg–AlN composite after 4 h reaction (gas flow rate: 0.6 lpm).

4. Discussion

The important thermodynamically feasible reactions [21] that can occur in the present study at 1173 K and the standard Gibbs energy change (ΔG°) of the reactions are as follows:

$$2Al_{(l)} + N_{2(g)} \rightarrow 2AlN_{(s)}, \qquad \Delta G_{(1)}{}^\circ = -382.9\,\mathrm{kJ} \tag{1}$$

$$3Mg_{(l)} + N_{2(g)} \rightarrow Mg_3N_2, \qquad \Delta G_{(2)}{}^\circ = -222.7\,\mathrm{kJ} \tag{2}$$

It is seen from Eqs. (1) and (2) that both reactions are thermodynamically feasible, however, nitridation of aluminium is more favorable than magnesium. When oxygen exists in the system, in addition to reactions (1) and (2), oxygen could react with the molten aluminium and magnesium by the following reactions:

$$(4/3)Al_{(l)} + O_{2(g)} \rightarrow (2/3)Al_2O_3, \qquad \Delta G_{(3)}{}^\circ = -869.04\,\mathrm{kJ} \tag{3}$$

$$2Mg_{(l)} + O_{2(g)} \rightarrow 2MgO, \qquad \Delta G_{(4)}{}^\circ = -945.9\,\mathrm{kJ} \tag{4}$$

The standard Gibbs free energy change for reaction (3) is more negative compared to reactions (1) and (2) implying that oxidation reaction of aluminium is thermodynamically more favorable than nitridation of aluminium and magnesium. Hence, oxygen should be reduced as low as possible. Scholz and Greil [22] investigated the formation of Al–AlN composites by direct nitridation of Al–Mg–Si melt and studied the effect of oxygen impurities in the nitriding atmosphere. In their experiments, nitrogen gas was introduced above the alloy melt. It was found that significant AlN could not be formed under commercial N_2 atmosphere but was formed under flowing high purity N_2 atmosphere. Swaminathan et al. [23] studied the influence of oxygen impurities on the formation of Al–AlN composites by infiltration method. They found that increasing oxygen content decreased the nitride content in the matrix. All these evidenced the deleterious effect of trace oxygen on nitridation of aluminium. Since in the present study high purity nitrogen gas was used, the effect of oxygen is expected to be minimum.

It has been reported that [21] Mg could getter oxygen in the Al–Mg–N–O system and so in the present study with Mg addition, it can react with oxygen by reaction (4). The standard Gibbs free energy change for reaction (4) is more negative compared to reaction (3) implying that Mg has preference to getter oxygen than aluminium. Further, it has been observed in the present work with Mg addition and 4 h reaction time with the higher flow rates of nitrogen a white colored powder was found to adhere at the internal walls and the top of the mild steel container. This has been identified as MgO by XRD (Fig. 11). This can possibly occur according to reaction (4) and due to the presence of higher amounts of oxygen. It has been reported [24] that the alloying element Mg plays a critical role in preventing the formation of a protective layer of

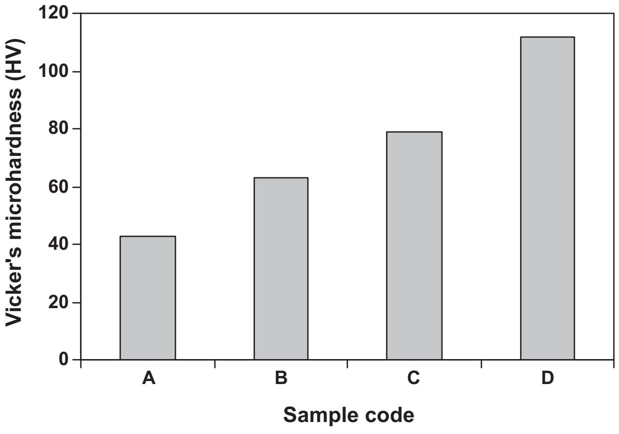

A = Pure Al^{27} ; B = Al-AlN (reaction time: 2 hours, gas flow rate: 0.4 lpm)
C = Al-4Mg-AlN (reaction time: 4 hours, gas flow rate: 0.4 lpm)
D = Al-4Mg-AlN (reaction time: 4 hours, gas flow rate: 0.6 lpm)

Fig. 10. Comparison of microhardness of in situ Al–AlN composites with pure Al.

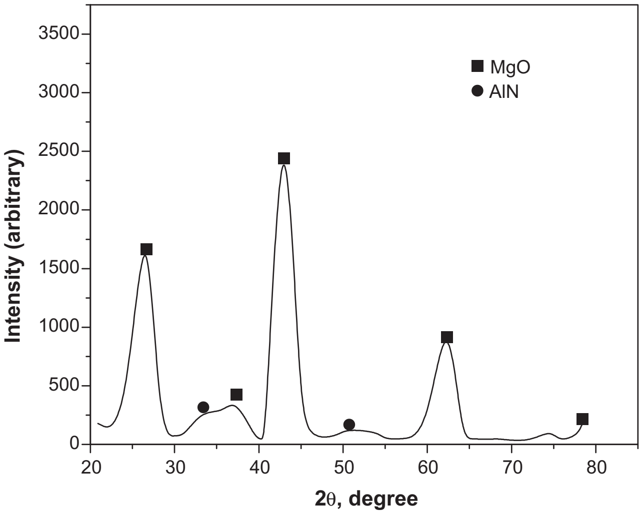

Fig. 11. XRD pattern of the white powder on the top of the mild steel case.

alumina on the surface of the melt and in enhancing the wetting of solid surface. Further, magnesium present in the alloy is reported to have a catalytic effect on nitride formation such that it helps to transfer the surface reaction into a volume reaction [22].

The mechanism of AlN formation in the process of gas/melt reaction has not been well explained. Hou et al. [6] proposed an indirect nitridation mechanism accordingly, magnesium nitride first forms in the vapor phase by the reaction of vaporized magnesium and nitrogen gas followed by incorporation of magnesium nitride particles into the molten aluminium, and fine aluminium nitride forms via an in situ substitution reaction between magnesium nitride and aluminium. The size of AlN particles is dependent on the size of the precursor Mg_3N_2 particles. Further, according to Hou et al. [6], when there was bulk nitridation, there was always greenish-yellow powder on the ingot surface, which is the characteristic color of magnesium nitride. Jin et al. [25] proposed that the formation of AlN is achieved via the reaction of aluminium with Si_3N_4, which is formed via the reaction of Si in aluminium and nitrogen prior to the formation of AlN, that is, Si acts as a catalyzer for the formation of AlN. From the thermodynamic viewpoint, nitridation of either Al or Mg is very favorable and strongly exothermic. Also AlN has higher thermal stability than magnesium nitride over the entire temperature range. Kinetically, however, the formation of magnesium nitride is a much more favorable reaction than that of aluminium nitride, above 1373 K in the vapor phase [6]. The authors believe that in the present study, the nitridation of aluminium melt takes place by direct route wherein the upward moving gas bubbles react with the Al melt at the interface forming AlN. As the AlN forms inside the melt, the viscosity of the melt is also increased which traps more bubbles and increase the residence time of the gas bubbles inside the melt thereby having more time to react with the Al surface forming more amount of AlN. Since MgO is formed (identified by XRD) on the top surface and walls of the mild steel case, and Mg_3N_2 is not detected in the present study, AlN could not have been formed by the indirect reaction as proposed by Hou et al. [6]. The authors' explanation is further supported from the work of Huashun et al. [26] who have also deduced the nitridation mechanism as, AlN will be formed by the direct reaction of Al with nitrogen gas in the melt during gas injection.

Microstructural observations by SEM and TEM show that the morphology of the particles was hexagonal. The size of the AlN particles was found to be in the range from nano, submicron to a few microns. XRD analysis of the extracted particles confirmed the formation of AlN in the melt. Further, it has been observed in the present work that the particles are interconnected and seen as network of particles in the grain boundaries at longer reaction times and with Mg addition. This may be due to the fact that, since the particles being very small, pushed to the grain boundaries (Fig. 3). Since most of the AlN particles formed are in nano and submicron size (Figs. 4 and 7), as soon as the AlN forms it gets agglomerated forming interconnected AlN. This interconnected AlN structure has also been reported by Hou et al. [6] and Daniel and Murthy [19].

Hardness of the composite is significantly increased by the hard AlN particles. The addition of ceramic reinforcements to Al matrix leads to modifications in the matrix properties. This leads to higher hardness in the composites. These hard AlN particles act as a barrier to dislocation flow in aluminium matrix. Hence, an increase in the volume fraction of the AlN particles in the aluminium matrix would tend to increase the magnitude of resistance offered to the motion of dislocations and thus higher measured micro-hardness.

5. Conclusions

(a) In situ Al–AlN composite with and without Mg addition was synthesized by nitrogen gas bubbling method.
(b) The morphology of the particles was found to be hexagonal by SEM and TEM. The size of the AlN particles was found to be in the range from nano, submicron to a few microns. XRD analysis of the extracted particles confirmed the formation of AlN in the melt.
(c) Presence of Mg enhanced the nitridation rate and formed network of interconnected AlN particles.
(d) Hardness of the composite is significantly increased due to the presence of hard AlN particles.
(e) The AlN particles formed are seen to be agglomerated in the microstructure and the challenge is to obtain uniformly distributed particles without agglomeration. Further work is required to obtain uniformly distributed particles by modifying the melt chemistry, experimental set-up and solidification conditions. Furthermore, correlation of the microstructural variables with the mechanical properties of the in situ Al–AlN composites produced by this method need to be studied in detail.

Acknowledgements

The authors thank the Council of Scientific and Industrial Research, New Delhi, for the award of Research Associate Fellowship to the first author, Mr. S.G.K. Pillai for optical metallography, Mr. Chandran for SEM and Mr. Antony, Mr. Riyas, Mr. Suresh, and Mr. V.P. Mahesh for their support during the work.

References

[1] B.S.S. Daniel, V.S.R. Murthy, G.S. Murty, J. Mater. Process. Technol. 68 (1997) 132–155.
[2] M.J. Koczak, K.S. Kumar, US Patent no. 4,808,372 (1989).
[3] P. Sahoo, M.J. Koczak, Mater. Sci. Eng. A 131 (1991) 69–76.
[4] P. Sahoo, M.J. Koczak, Mater. Sci. Eng. A 144 (1991) 37–44.
[5] M.K. Premkumar, M.G. Chu, Mater. Sci. Eng. A 202 (1995) 172–178.
[6] Q. Hou, R. Mutharasan, M. Koczak, Mater. Sci. Eng. A 195 (1995) 121–129.
[7] C.X. Cui, R.J. Wu, Y.C. Li, Y.T. Shen, J. Mater. Process. Technol. 100 (2000) 36–41.
[8] R.F. Shyu, F.T. Weng, C.T. Ho, J. Mater. Process. Technol. 122 (2002) 301–304.
[9] A. Khatri, M. Koczak, Mater. Sci. Eng. A 162 (1993) 153–162.
[10] K. Seon Shin, Y.-S. Kim, N.J. Kim, CAAM Report 98001F, April 1998.
[11] W. Werdecker, F. Aldinger, US Patent no. 4,377,425, March 22 (1983).
[12] M.K. Aghajanian, J.P. Biel, R.G. Smith, J. Am. Ceram. Soc. 77 (1994) 1917–1920.
[13] F. Jean, M. Haussonne, Mater. Manuf. Proc. 10 (1995) 717–755.
[14] Q. Zheng, B. Wu, R.G. Reddy, Adv. Mater. Eng. 5 (2003) 167–172.
[15] Q. Zheng, R.G. Reddy, B. Wu, Proceedings of the Conference on 'State of the Art in Cast MMC's TMS Fall Meeting', Warrendale, St. Louis, Missouri, USA, 2000, pp. 1–12.
[16] Q. Zheng, R.G. Reddy, Proceedings of the Conference on 'Affordable Metal–Matrix Composites for High Performance Applications', TMS, Indiana, USA, 2001, pp. 199–210.

[17] Q. Zheng, R.G. Reddy, Proceedings of the Conference on ‘NSF Design, Service and Manufacturing Grantees and Research Conference’, Iowa State University, Ames, Iowa, USA, 2002, pp. 2144–2146.

[18] Q. Zheng, R.G. Reddy, Proceedings of the Conference on ‘NSF Design, Service and Manufacturing Grantees and Research Conference’, The University of Alabama, Tuscaloosa, AL, USA, 2003, pp. 2262–2266.

[19] B.S.S. Daniel, V.S.R. Murthy, Mater. Des. 16 (1995) 155–161.

[20] M. Gupta, L. Adi, V.V. Ganesh, T.S. Srivatsan, Curr. Sci. 88 (2005) 1419–1425.

[21] Q. Zheng, R.G. Reddy, High Temp. Mater. Process. 22 (2003) 63–71.

[22] H. Scholz, P. Greil, J. Mater. Sci. 26 (1991) 669–677.

[23] S. Swaminathan, B.S. Rao, V. Jayaram, Mater. Sci. Eng. A 337 (2002) 134–139.

[24] M.K. Aghajanian, M.A. Rocazella, J.T. Burke, J. Mater. Sci. 26 (1991) 447–454.

[25] H. Jin, K. Chen, H. Zhou, Y. Wang, Z. Zou, W. Wang, Acta Metall. Sin. 36 (2000) 775–779.

[26] Y. Huashun, J.D. Kim, S.B. Kang, Mater. Sci. Eng. A 386 (2004) 318–325.